# Operational Report of the Mission Analysis and Planning System for the KOMPSAT-I

Byoung-Sun Lee, Jeong-Sook Lee, Jae-Hoon Kim, Seong-Pal Lee,
Hae-Dong Kim, Eun-Kyou Kim, and Hae-Jin Choi

**Since its launching on 21 December 1999, the Korea Multi-Purpose Satellite-I (KOMPSAT-I) has been successfully operated by the Mission Control Element (MCE), which was developed by the ETRI. Most of the major functions of the MCE have been successfully demonstrated and verified during the three years of the mission life of the satellite. This paper presents the operational performances of the various functions in MAPS. We show the performance and analysis of orbit determinations using ground-based tracking data and GPS navigation solutions. We present four instances of the orbit maneuvers that guided the spacecraft from injection orbit into the nominal on-orbit. We include the ground-based attitude determination using telemetry data and the attitude maneuvers for imaging mission. The event prediction, mission scheduling, and command planning functions in MAPS subsequently generate the spacecraft mission operations and command plan. The fuel accounting and the realtime ground track display also support the spacecraft mission operations.**

**Keywords: Satellite operation, mission analysis, mission planning, orbit attitude, KOMPSAT.**

Manuscript received September 30, 2002; revised July 3. 2003.

This work was supported by the Ministry of Information and Communication of Korea.

Byoung-Sun Lee (phone: +82 42 860 4903, email: lbs@etri.re.kr), Jeong-Sook Lee (email: jsooklee@etri.re.kr), Jae-Hoon Kim (email: jhkim@etri.re.kr), and Seong-Pal Lee (email: spallee@etri.re.kr) are with Radio & Broadcasting Research Laboratory, ETRI, Daejeon, Korea.

Hae-Dong Kim (email: haedkim@kari.re.kr), Eun-Kyou Kim (email: ekkim@kari.re.kr), and Hae-Jin Choi (email: hjchoi@kari.re.kr) are with Satellite Mission Operations Group, KARI, Daejeon, Korea.

## I. Introduction

The Korea Multi-Purpose Satellite-I (KOMPSAT-I) was successfully launched by the Taurus launch vehicle at 07:13:00 UTC, 21 December 1999, from Vandenberg Air Force Base, California, U.S.A. Since then, the spacecraft has been successfully operated by the KOMPSAT Ground Station (KGS) located in the Korea Aerospace Research Institute (KARI) in Daejeon, Korea. The main mission of the KOMPSAT-I was to perform cartography of the Korean peninsula during the design life of three years. The secondary mission was to take large-scale multi-spectral images of the ocean. The other science missions were ion layer measurement and high-energy particle detection.

The KGS consists of the Mission Control Element (MCE) and the Image Reception and Processing Element (IRPE). The IRPE is responsible for collecting and processing image data from the satellite. The MCE is used for satellite mission control, such as tracking, telemetry reception and processing, command planning and transmission, mission analysis and planning, and anomaly resolution [1].

Most of the major functions in the MCE have been performed and verified during the more than three years of the mission control operation of the KOMPSAT-I. These functions include Launch and Early Orbit Phase (LEOP) operations and on-orbit normal phase operations.

This paper presents the operational performances of the various functions in MAPS. For the LEOP and on-orbit operations, we demonstrate the orbit related functions, such as orbit determination, orbit prediction, and orbit maneuver, and for the imaging operations, we demonstrate the attitude-related functions, such as attitude determination and attitude maneuver.

We explain the mission planning functions, including event prediction, mission scheduling, and command planning for the spacecraft mission operations. We validate the support functions, such as fuel accounting and realtime ground track display for the KOMPSAT-I mission control.

## II. The Mission Control Element for the KOMPSAT-I

The MCE is made up of four subsystems: Tracking, Telemetry and Command subsystem (TTC); Satellite Operations Subsystem (SOS); Mission Analysis and Planning Subsystem (MAPS); and satellite Simulator subsystem (SIM). The MCE receives telemetry from the satellite and sends telecommands via the S-band link. The data format for the telemetry and telecommands takes the standard form of the Consultative Committee for Space Data Systems (CCSDS). Figure 1 shows the schematics of the MCE. TTC receives telemetry from the satellite, transmits telecommands, and tracks the signals of the satellite. The SOS provides telemetry data processing, telecommand generation, and telecommand transmission to the TTC or to SIM [2]. The MAPS analyzes the orbit and attitude of the KOMPSAT-I and plans the mission schedule and command sequence [3], [4]. The SIM validates telecommands, simulates the spacecraft, analyzes anomalies, and is used for training the mission control operators [5], [6].

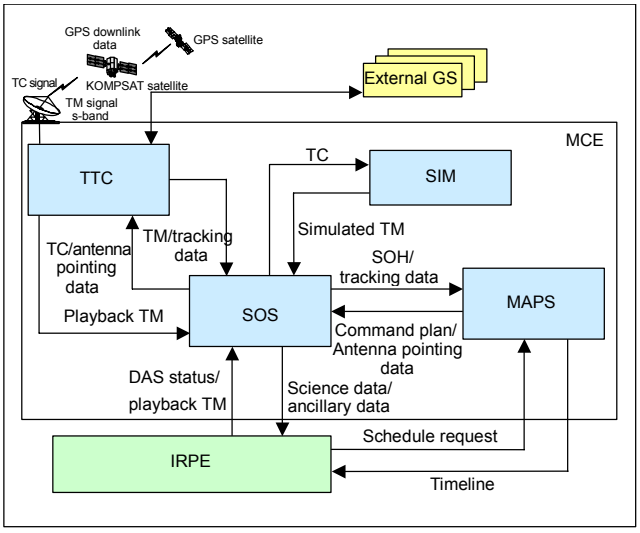


Fig. 1. Schematics of the KOMPSAT-I MCE.

The MAPS includes the functions of orbit determination and prediction as well as orbit maneuver planning using satellite-tracking data. The MAPS also performs ground-based attitude determination and prepares spacecraft attitude maneuver plans for the image data collection of the specific area. The MAPS generates conflict-free monthly, weekly, and daily satellite operation schedules and mission timelines. The MAPS consists of five blocks: the System Management Block (SMB), Mission Planning Block (MPB), Orbit Determination and Prediction Block (ODPB), Orbit Maneuver Block (OMB), and Attitude Maneuver and Determination Block (AMDB). Support and utility functions include realtime ground track display and osculating-to-mean orbit conversion. Figure 2 shows the functional block diagram of the MAPS.

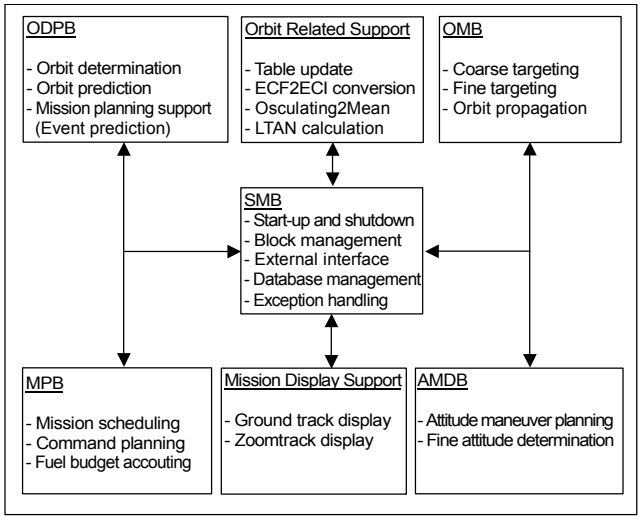


Fig. 2. Functional block diagram of the MAPS.

## III. Orbit Determination (OD)

### 1. OD Using Ground-Based Tracking Data

Six S-band tracking stations participated in the KOMPSAT-I LEOP operations. The German Space Operations Center (GSOC) station was directly linked to the KGS for telemetry monitoring and command transmission. Predicted antenna pointing data for the GSOC station were generated based on the state vector provided by the KGS. Four NASA tracking stations–McMurdo (MGS), PokerFlat (PKF), Svalbard (SGS), and Wallops (WGS)–were linked to the GSOC station.

Figure 3 shows a ground trace of the KOMPSAT-I from injection for 24 hours. The figure also shows the ground coverages of the tracking stations and the satellite. The shadowed area over the European countries represents the area of eclipse in the satellite altitude. The support function of the MAPS, i.e., the realtime ground track display, is used for generating the KOMPSAT-I trace.

The first operational OD for the KOMPSAT-I in KGS was performed on the second day of the launch. Prior to the first OD in the KGS, the two-line-element (TLE) from NORAD was used for antenna pointing. Angle tracking and ranging data from four stations were collected on the second day of the

launch and used for the OD. Normally, two or three days ranging data were collected and used for the OD. In this case, the angle tracking and ranging data of only one day was used for the first operational OD.

On the second day of the launch, 14 tracking data files were collected from the four tracking stations. The ranging data from the KGS and GSOC had a two-way range and two-way Doppler, whereas the range rate data from the SGS and PKF stations were one-way Doppler. The commands from the KGS activated the two-way ranging while the one-way Doppler measurement data were collected independently by the tracking station without ground commands to the spacecraft.

Various OD solutions were derived and analyzed using different combinations of the tracking stations and measurement data types. Table 1 shows the OD results using one-day data. In all cases except the GSOC, the data converged to the 5% criteria within 9 iterations. Only in the GSOC did the OD fail after 9 iterations and give a wrong orbit. OD using KGS data shows a faster convergence. OD using all measurement data from the KGS was used as a reference in Table 1 for evaluation of the OD differences.

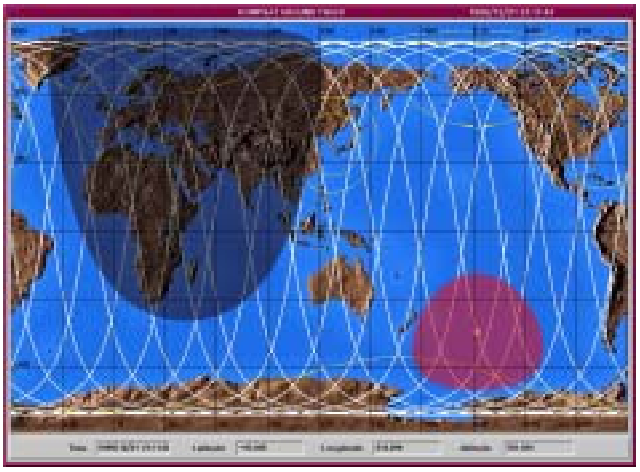

Fig. 3. KOMPSAT-I ground trace and station coverage.

Table 2 presents the measurement data statistics in the OD process for the KGS and GSOC. All data below 5 degrees of elevation angle were rejected by elevation cut-off criteria. All measurement data types from the KGS showed good integrity. However, much of the range and range rate data from the GSOC were rejected in the OD process. There seemed to be a calibration problem in the satellite ranging process, so only the ranging data from the KGS were used for OD after that time.

In order to analyze the integrity of the OD using the KGS data, two consecutive ODs were performed for the overlapping period. Measurement data from five passes between 22 and 23 December 1999 were used. The first three sets of ranging data were used for the first OD, and the last three sets of ranging data were used for the next OD, so one set of ranging data was commonly used for two ODs. The last two measurement data sets included only antenna angle data. Figure 4 shows the position and velocity differences for the overlapping period in the two consecutive ODs. Although a small amount of the ranging data set was processed, the differences were relatively small enough to use the OD solution for antenna pointing. In addition, we made a comparison in a separate way between the

Table 1. Orbit determination results using one-day data (epoch: 22 December1999 00:00:00 UTC).

| Stations | KGS only | GSOC only | KGS GSOC | KGS GSOC SGS PKF | KGS only | KGS GSOC | KGS GSOC SGS PKF |
|---|---|---|---|---|---|---|---|
| Data type | All data | All data | All data | All data | Range rate | Range rate | Range rate |
| Converge* | Convg. (4) | Fail (9) | Convg. (9) | Convg. (9) | Convg. (4) | Convg. (6) | Convg. (6) |
| $a$ (km) | 7088.797 | 7136.464 | 7088.926 | 7088.916 | 7088.796 | 7088.911 | 7088.911 |
| $e$ (-) | 0.0029104 | 0.255495 | 0.0032551 | 0.0031383 | 0.0029098 | 0.0030228 | 0.0030226 |
| $i$ (deg) | 98.25863 | 99.07964 | 98.28709 | 98.27718 | 98.25837 | 98.29367 | 98.29376 |
| $\Omega$ (deg) | 251.74217 | 252.87396 | 251.76743 | 251.75781 | 251.74195 | 251.78016 | 251.78026 |
| $\omega$ (deg) | 193.87414 | 168.87754 | 184.28977 | 185.42725 | 193.88692 | 185.47128 | 185.43971 |
| $M$ (deg) | 1.77707 | 31.78406 | 11.45294 | 10.29954 | 1.76415 | 10.24542 | 10.27737 |
| $\Delta$ Position (km) | N/A | 796.5826 | 18.93135 | 15.81843 | 0.029034 | 14.14694 | 14.21491 |
| $\Delta$ Velocity (km/s) | N/A | 0.768185 | 0.016492 | 0.01356 | 4.51E-5 | 0.012656 | 0.012716 |

*Convg.: Converge (no. of iteration), Fail: Fail to converge (no. of iteration)

Table 2. Measurement data statistics in OD.

| Data | | KGS only | | GSOC only | | KGS+GSOC | |
|---|---|---|---|---|---|---|---|
| | | Applied | Accepted | Applied | Accepted | Applied | Accepted |
| KGS | Azimuth | 842 | 747 | | | 842 | 747 |
| | Elevation | 842 | 741 | | | 842 | 747 |
| | Range | 480 | 480 | | | 480 | 300 |
| | Range rate | 540 | 539 | | | 540 | 305 |
| GSOC | Azimuth | | | 3,407 | 2,405 | 3,407 | 3,206 |
| | Elevation | | | 3,407 | 1,922 | 3,407 | 3,206 |
| | Range | | | 284 | 13 | 284 | 47 |
| | Range rate | | | 2,605 | 16 | 2,605 | 529 |
| | Total | 2,704 | 2,507 | 9,703 | 4,356 | 12,407 | 9,089 |

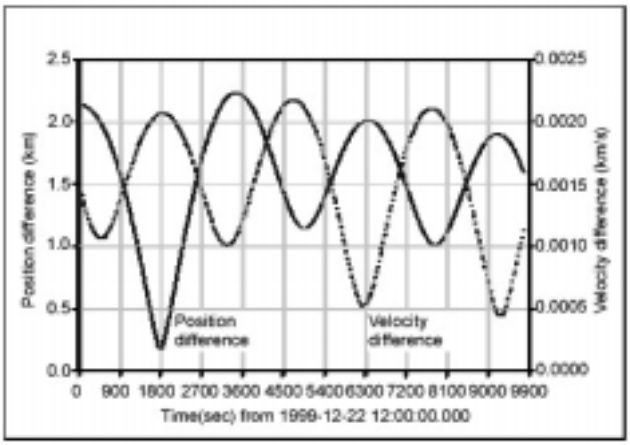


Fig. 4. Position and velocity difference for the overlapping period in two consecutive ODs.

OD using the KGS data and SGP4 propagation [7] from the NORAD TLE. The difference between the two orbits was also small enough to use the OD solutions in the LEOP mission operations. For the KOMPSAT-I mission operations, we used the OD using only the KGS data until the onboard GPS receiver was switched on.

## 2. OD Using GPS Navigation Solutions

OD for the KOMPSAT-I using GPS navigation solutions was carried out after the onboard GPS receiver was switched on [8]. The first GPS navigation solutions were gathered on 25 December via realtime telemetry. Then playback GPS navigation solutions were gathered on 26 December. At that time, the GPS replacement option was turned off, so only the earth-centered-fixed position and velocity data in every 32-second interval from the GPS receiver was used for the OD. A Motorola Viceroy GPS receiver was mounted on the KOMPSAT-I, and it used a C/A code on a GPS L1 frequency to provide the earth-centered-fixed position, velocity, and time [9]. When the GPS replacement option was turned on, the earth-centered-inertial (ECI) position and velocity data from the onboard computer could be collected. There are three possible options for OD using position and velocity data from the onboard GPS receiver: use of position data only, velocity data only, or position and velocity data.

The totals of 1850 sets of position and velocity data were used for the OD. Each component in the position and velocity vector was used as one measurement of data in the OD process. A priori data of the orbit on 25 December were used for the OD. An a priori orbit was determined using 283 sets of realtime GPS navigation solutions during the period of 25 December to 26 December. The NORAD TLE near the orbit epoch of 26 December 1999 at 08:50 was used for the comparison of the OD results.

All three ODs converged to 5% of the convergence criteria within 7 iterations. Many iterations were required due to the bad quality of the a priori data. The options for the measurement data such as position and velocity made little impact on the OD results. Faster convergence was achieved when position only or velocity only measurement data were used. Measurement data rejection rates were different according to the combinations of the measurement data. Position only measurement data showed the smallest rejection rates. Table 3 shows the differences of the OD results among the three cases. The result for the position only measurement data is close to the position and velocity cases. The differences arising from the combination of the measurement data mainly came out as along-track errors. The time difference of the NORAD TLE results was less than 1.5 seconds compared to

Table 3. Comparison of the OD (Epoch : 26 December 1999 08:50:00.000 UTC).

| Differences | Case 1 – Case 2 | Case 1 – Case 3 | Case 2 – Case 3 | Case 1 – TLE |
|---|---|---|---|---|
| $\Delta a$ (km) | 0.001 | −0.001 | −0.002 | 0.11462 |
| $\Delta e$ (-) | −2.0E−06 | −1.9E−06 | 1.0E−07 | −0.00014 |
| $\Delta i$ (deg) | 0.00043 | 0.00029 | −0.00014 | −0.00039 |
| $\Delta \Omega$ (deg) | 0.00036 | −0.00139 | −0.00175 | −0.00547 |
| $\Delta \omega$ (deg) | −0.08224 | −0.05915 | 0.02309 | −2.3028 |
| $\Delta M$ (deg) | 0.08461 | 0.07039 | −0.01422 | 2.38478 |
| $\Delta (\omega + M)$ (deg) | 0.00237 | 0.01124 | 0.00887 | 0.08198 |
| Δ Radial (km) | −0.031 | −0.028 | 0.003 | −1.128 |
| Δ Along-track (km) | 0.275 | 1.411 | 1.136 | 10.810 |
| Δ Cross-track (km) | −0.001 | 0.157 | 0.158 | 0.501 |

*Case 1: position + velocity, Case 2: position only, Case 3: velocity only

the OD using GPS navigation solutions. Since then, all the mission operations in LEOP were successfully performed with the OD using GPS navigation solutions.

The orbit in Case 1 was propagated with a 32-second interval for the comparison between the OD results and the GPS navigation solutions. Figures 5 and 6 show the ECI position and velocity vector difference. The totals for 1845 data points were compared because 5 sets of GPS navigation solutions were all zeros. This was due to an anomaly in the GPS receiver. The figures show wide noise ranges of the GPS navigation solutions. Table 4 presents the statistics of the difference. The results show that one point of the GPS navigation solution should not be used as the orbital state for the satellite operation. The OD process should be performed using many sets of GPS navigation solutions.

The accuracy of the GPS navigation solutions was affected by many factors, including selective availability (SA), which is the intentional degradation of the GPS ephemerides. Point positioning with the GPS was as accurate in the low earth orbit as on the ground, typically 50–100 m for the GPS standard positioning service user under nominal levels of selective availability, and a corresponding velocity accuracy of about

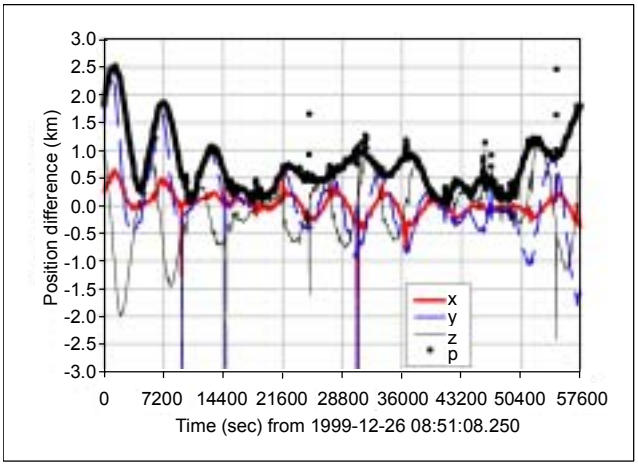


Fig. 5. Position vector difference.

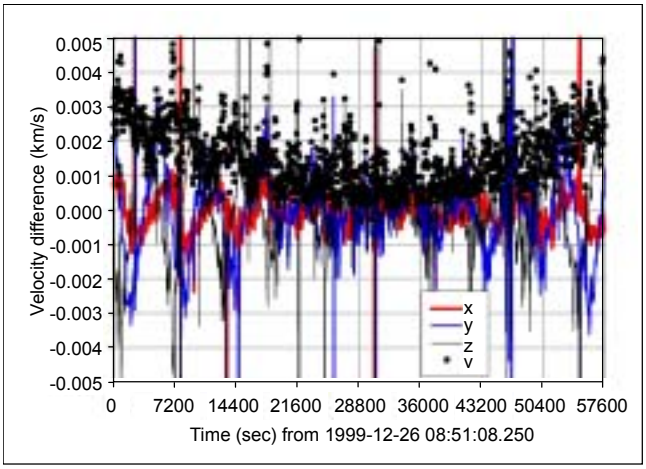


Fig. 6. Velocity vector difference.

Table 4. Statistics of the difference between OD results and GPS navigation solutions.

| | Mean | Standard deviation | Maximum | Minimum |
|---|---|---|---|---|
| Δ Position (km) | 0.782 | 0.618 | 7.973 | 0.0259 |
| Δ Velocity (km/s) | 0.00192 | 0.00509 | 0.19900 | 0.00006 |

0.5 m/s [10]. The capability for orbit prediction was severely limited by the GPS standard positioning service velocity accuracy of about 0.5 m/s, which is equivalent to a 1 km error in the semi-major axis [11].

At approximately 04:05 UTC on 2 May 2000, the U.S. government stopped its SA, which is the intentional degradation of the civilian GPS signal that is used to protect military operations [12]. The accuracy of the GPS navigation solutions improved after the termination of the SA. We studied KOMPSAT-I GPS navigation solutions and the following OD during the SA transition period [13]. Figure 7 shows the osculating semi-major axis of the KOMPSAT-I GPS navigation solutions during the SA transition period. The vertical centerline in the figure is the reference time for the SA transition. The scattering of the semi-major axis (SMA) after SA was turned off was smaller than that before the SA was turned off. The sharp peak pattern in the ridges of the semi-major axis variation seemed to be introduced by a GPS satellite configuration or receiver problem.

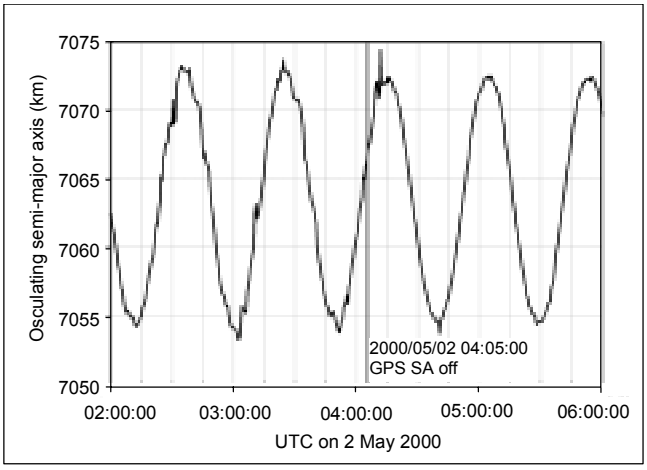


Fig. 7. Osculating semi-major axis variations with and without SA.

OD using 1-day GPS navigation solutions before and after the SA was turned off were performed for the analysis of the SA effects. Position and velocity data in GPS navigation solutions were used. Figures 8 and 9 show the OD residuals of the SMA before and after the SA was turned off. The residuals were defined as the difference between the OD results and the GPS navigation solutions. The figures clearly show that the residuals with the SA off were smaller than those with the SA on.

## IV. Orbit Maneuver (OM)

Although the injection orbit of the KOMPSAT-I was within the allowable tolerances of the Taurus launch vehicle, the size

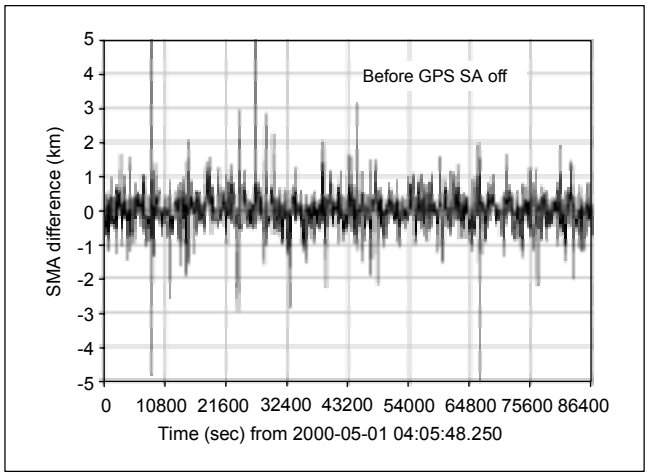


Fig. 8. SMA residuals in OD with SA on.

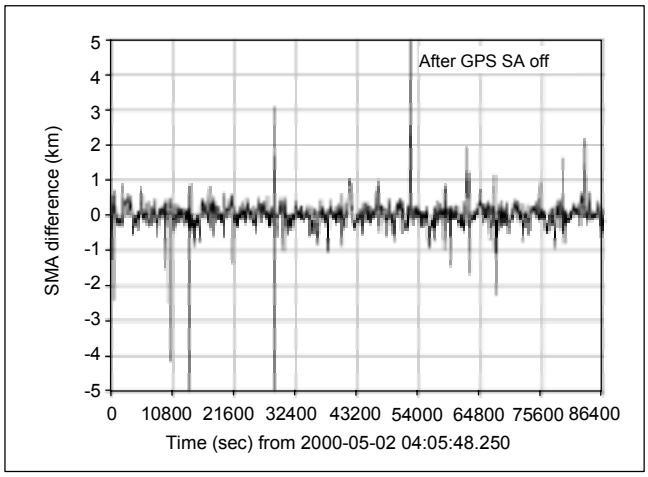


Fig. 9. SMA residuals in OD with SA off.

of the orbit was somewhat larger than that of the nominal size, and the inclination of the orbit was greater than that of the nominal inclination. Therefore, both in-plane and out-of-plane maneuvers were required to achieve the nominal orbit. Extensive post-launch mission analysis was performed after the launch [14]. Table 5 shows the comparison of the target orbit and the realized injected orbit of the KOMPSAT-I. All of the parameters are within the allowable tolerances as specified in the Taurus T4 Interim Mission Analysis document [15].

A series of orbit maneuvers were performed after the completion of the critical spacecraft checkout. Two in-plane orbit maneuvers (IPM) and two out-of-plane orbit maneuvers (OPM) were planned and executed for reducing the orbital size and inclination. Table 6 shows the orbit maneuver planning parameters for the four maneuvers. The last line in Table 6 shows the maneuver realization. Since the four thrusters of the KOMPSAT-I were directed to the zenith direction in the normal cruising attitude, ±90 degrees of pitch or roll attitude

Table 5. Comparison of the target orbit and realized orbit.

| Parameters | Target by OSC | Realized | Difference |
|---|---|---|---|
| Osculating injection apse (km) | 7069.2 ± 10 | 7068.414 | −0.786 |
| Osculating opposite apse (km) | 7075.7 ± 50 | 7112.029 | +36.329 |
| Osculating inclination (deg) | 98.125 ± 0.15 | 98.2670 | +0.142 |
| Mean injection apse (km) | 7063.275 ± 10 | 7062.396 | −0.879 |
| Mean opposite apse (km) | 7063.275 ± 50 | 7099.902 | +36.627 |
| Mean inclination (deg) | 98.13 ± 0.15 | 98.2733 | +0.1433 |
| Mean LTAN* (hh:mm:ss) | 10:50 AM ± 5 min | 10:46:34 | −03:26 |

*LTAN: local time of ascending node

Table 6. Orbit maneuver planning and realization.

| Maneuver number | 1st IPM | 1st OPM | 2nd OPM | 2nd IPM |
|---|---|---|---|---|
| Burn start time | 2000-01-01 23:37:22 | 2000-02-02 00:03:13 | 2000-02-08 23:58:20 | 2000-02-16 00:53:00 |
| Burn duration(sec) | 180.0 | 240.0 | 360.0 | 263.0 |
| Maneuver target | –10.708 km of SMA | –0.0398 deg of INC | –0.0475 deg of INC | -8.294 km of SMA |
| Event | GSOC contact | descending node | descending node | KGS contact |
| Attitude | Pitch –90 deg. | Roll 90 deg. | Roll 90 deg. | Pitch –90 deg. |
| Thruster calibration factor | 1.0 | 0.673 | 0.542 | 0.518 |
| Effective thrust (N) | 14.669 | 9.869 | 7.953 | 7.602 |
| Expected fuel used (kg) | 1.229 | 1.643 | 2.442 | 1.797 |
| Δ Velocity magnitude (m/s) | –5.615 | –5.160 | –6.098 | –4.327 |
| Maneuver realization | –7.185 km of SMA | –0.0321 deg of INC | –0.0451 deg of INC | –8.393 km of SMA |

maneuver was required for orbit maneuvers. During the thruster firings in the orbit maneuver, the satellite used each of the four thrusters in the off-pulse mode for attitude control. It was difficult for the ground mission control to estimate the duration of the off-pulse mode, so a parameter called the thruster calibration factor in Table 6 was applied for the orbit maneuver planning. After the orbit maneuvers, the thruster calibration factor was updated considering the maneuver realization, so the maneuver realization in the 2nd IPM was very close to the maneuver target.

Two IPMs were performed near the perigee point to reduce the size of the orbit (Table 6). The thruster firings of the two IPMs were monitored via a realtime telemetry link. Whereas two OPMs were executed in nodal crossings, no realtime telemetry was monitored in the KGS.

The orbit determination and maneuver evaluation were performed after maneuvers using GPS navigation solutions in playback telemetry. The thruster calibration factor was derived from matching the orbit determination results to the maneuver planning. The derived thruster calibration factor was used for the next maneuver planning. As Table 6 shows, the first three thruster firings were under-shut and the last thruster firing was slightly over-shut. The thruster calibration factor converged. Figures 10 to 13 show the orbital element variation during the thruster firing. The orbital elements were derived from GPS navigation solutions. No thrust values in the figures were generated by orbit propagation. Finally, the KOMPSAT-I achieved a nearly frozen orbit in the nominal altitude by the 2nd IPM on 16 February 2000 [16].

## V. Attitude Determination and Attitude Maneuver

### 1. Attitude Determination Using Playback Telemetry Data

The MAPS can determine attitude using playback telemetry data from the spacecraft. The Kalman filter algorithm was

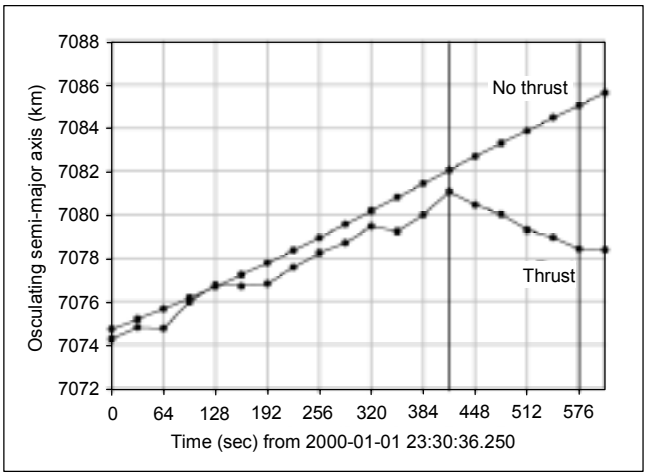


Fig. 10. SMA variations during the 1st IPM.

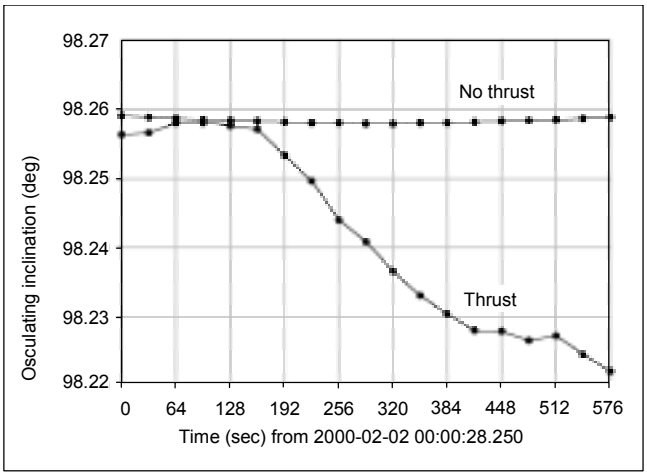


Fig. 11. INC variations during the 1st OPM.

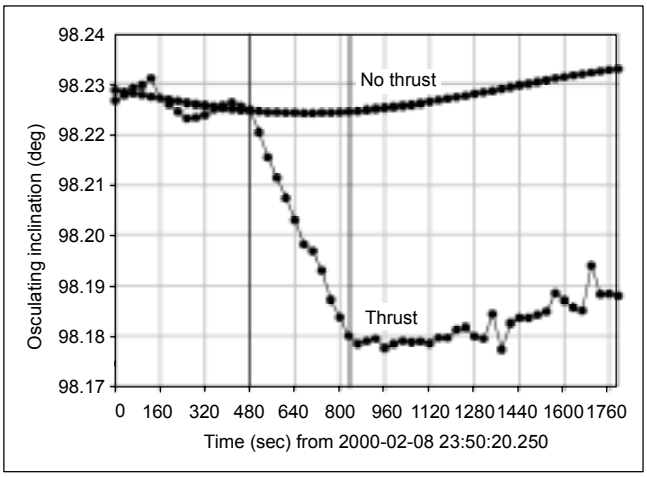


Fig. 12. INC variations during the 2nd OPM.

applied to the sequential ground attitude determination. Occasionally the ground attitude determination was performed for checking out the onboard attitude determination. Various

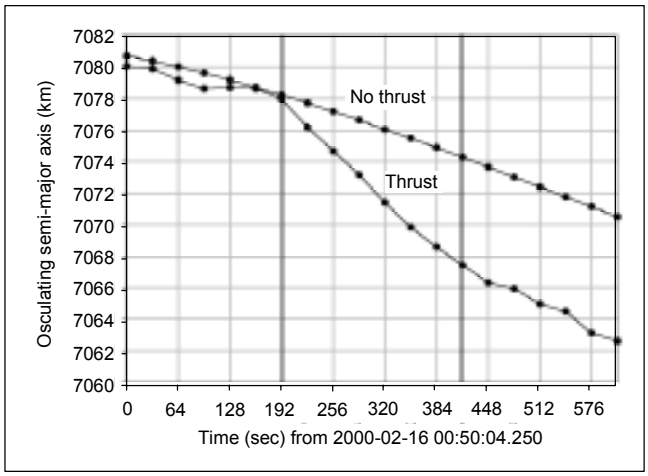


Fig. 13. SMA variations during the 2nd IPM.

measurements, such as a conical earth sensor, a fine sun sensor assembly, and Gyro data were used for the attitude determination.

The ground attitude determination using the MAPS was performed on the 18 January 2000 using the playback telemetry data from 17 January 2000 at 15:05:50 to 18 January 2000 at 02:05:03. Totals of 2472 conical earth sensor and fine sun sensor assembly data items were collected in the playback data. However, only 1226 of the conical earth sensor data items and 69 of the fine sun sensor assembly data items with valid flags were used for attitude determination. Although the data interval for conical earth sensor and fine sun sensor assembly data in telemetry was 16 seconds, the output interval for ground attitude determination was one second. Figures 14 to 16 show the attitude measurement and determination in roll, pitch, and yaw axis.

The attitude determination using the Kalman filter presents some sinusoidal continuity even though the raw measurement data from the sensors fluctuated greatly. Figure 17 shows the combined attitude errors in three axes.

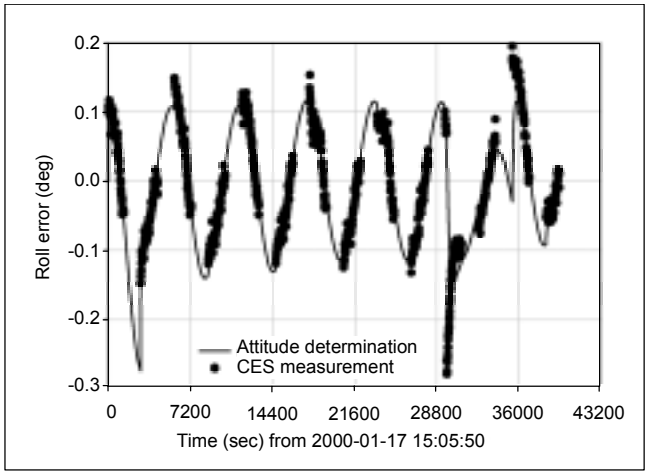


Fig. 14. Roll error variation.

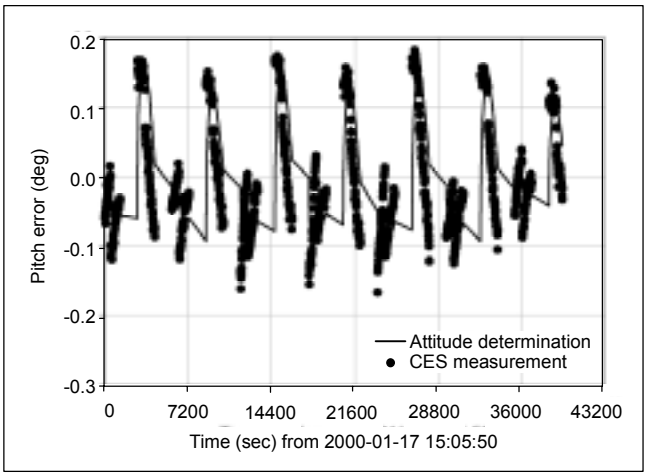


Fig. 15. Pitch error variation.

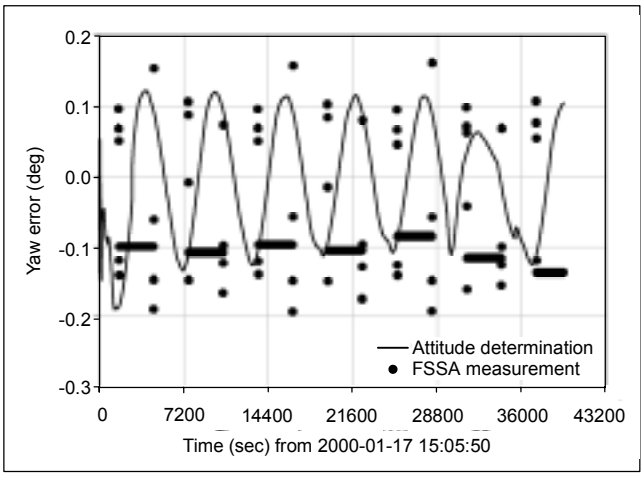


Fig. 16. Yaw error variation.

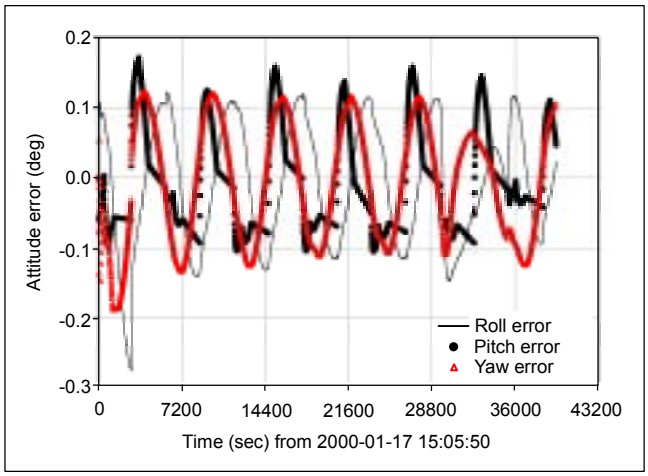


Fig. 17. Attitude error variation from attitiude determination.

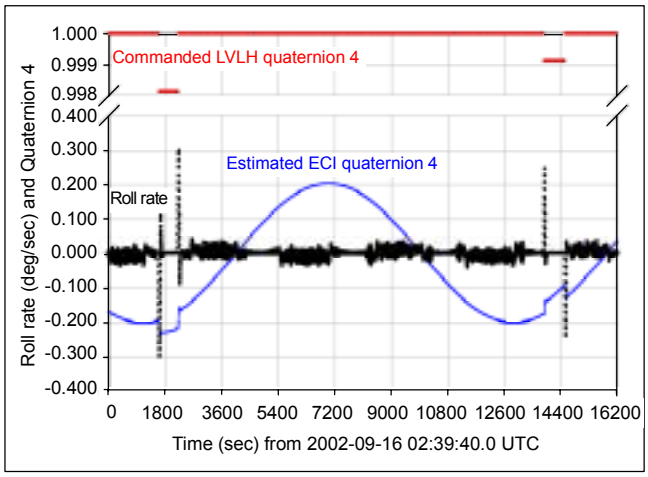


Fig. 18. Roll rate and quaternion 4.

## 2. Attitude Maneuver for Imaging

An attitude roll maneuver was performed for imaging when the ground target was not in the satellite ground track path. The required roll maneuver angles were re-calculated based on the imaging operation request from the IRPE. The solar array position angle in the middle of the imaging operation was also calculated because the solar array was fixed during imaging. The required roll angle was converted into the Local Vertical and Local Horizontal (LVLH) quaternion for commanding.

Figure 18 shows the commanded LVLH quaternion 4, estimated ECI quaternion 4, and roll rate for the two imaging operations. Playback telemetry data were used for plotting. The roll rate was abruptly changed by the commanded LVLH quaternion. The estimated ECI quaternion was discontinued by the commanded LVLH quaternion other than 1.0.

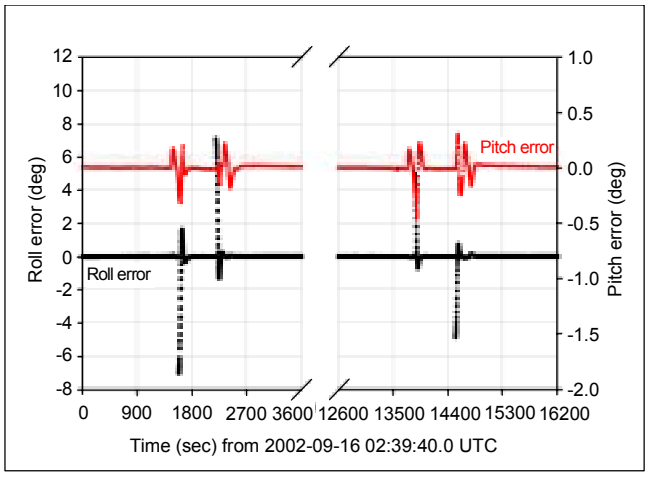


Fig. 19. Roll and pitch errors.

Figure 19 presents the roll and pitch errors during the roll maneuver operations for imaging. Roll and pitch angle errors

were caused by the difference between the commanded angle and the estimated angle. Pitch error was due to the attitude disturbance during the roll maneuver.

## VI. Mission Scheduling and Command Planning

Normal mission operations of the KOMPSAT-I were started after two months of LEOP operations. Mission scheduling and command planning was essential for normal spacecraft payload operations that included the electro-optical camera and ocean scanning multi-spectral imager. Mission scheduling consisted of daily, weekly, and monthly scheduling.

Orbital events such as Sun eclipse due to the Earth and Moon, nodal and apsidal crossing time, ground station contact time, sensor intrusion time, and Sun calibration time for the ocean scanning multi-spectral imager were generated by the event prediction program. Such orbital events were used as basic input for the mission scheduling. The electro-optical camera and ocean scanning multi-spectral imager, imaging requests, and spacecraft housekeeping requests, such as onboard time correction and ephemeris upload, were merged into the mission scheduling. After resolving the mission conflicts, the mission schedule was confirmed and used for generating the command plan. Spacecraft commands were transmitted when the satellite passed over the KGS. A sequence of the spacecraft commands for a specific mission was grouped as a relative timed command sequence [17].

Figure 20 shows a mission operation for the electro-optical camera and ocean scanning, multi-spectral imager imaging mission on 5 September 2002. The MAPS utility program, called Zoomtrack, was used for displaying the zoomed-in ground track and imaging area on the world map. Figure 21 presents the processed image of the Gangneung city area taken by the electro-optical camera as scheduled in Figure 20. The image data were received in the X-band link and processed by the IRPE [18].

## VII. Fuel Accounting

The KOMPSAT-I MAPS provides two types of methods for tracking the remaining fuel on board the spacecraft. One is a spreadsheet fuel budget analysis, and the other is a pressure,

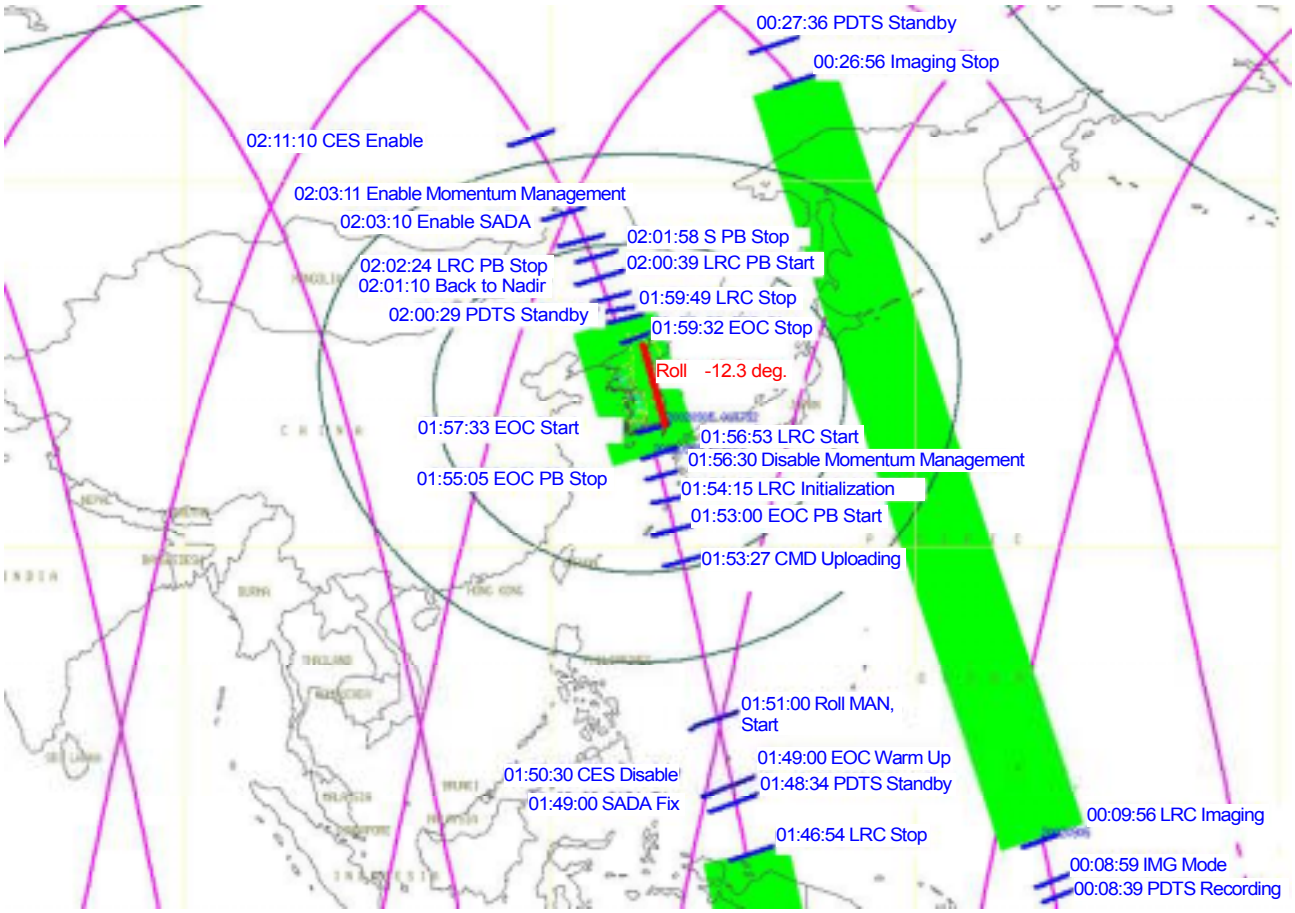


Fig. 20. Mission operations scenario with ground trace on the map.

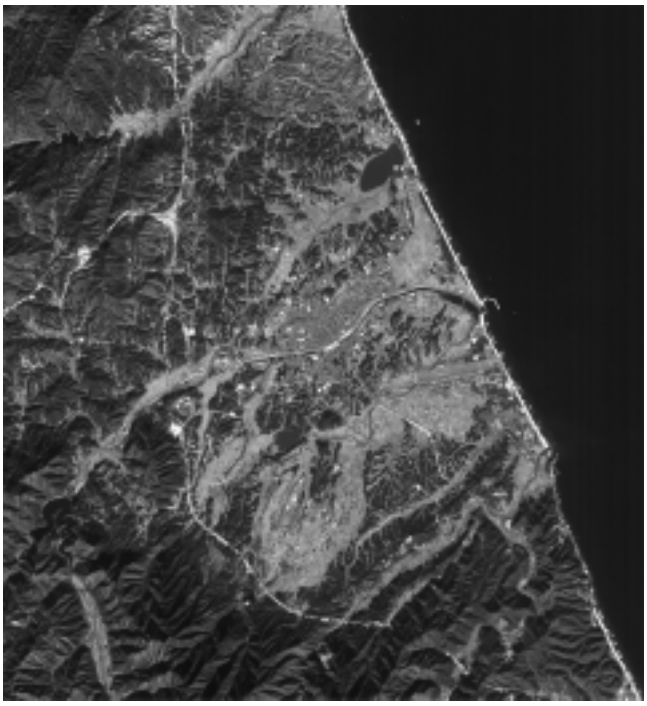

Fig. 21. Image taken by KOMPSAT-I (Gangneung city area on 5 September 2002).

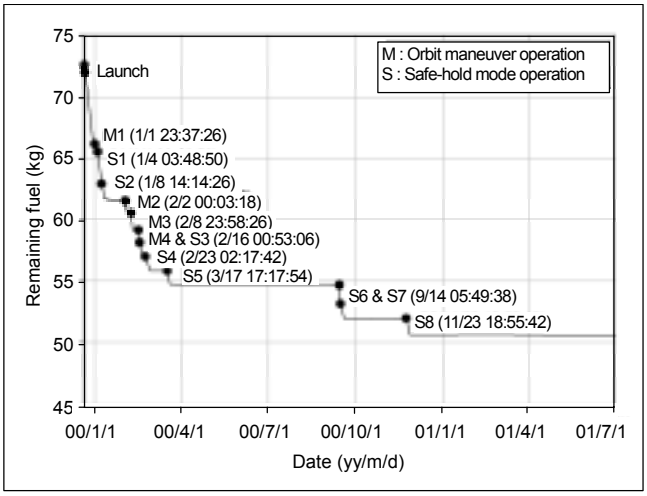


Fig. 22. Remaining fuel trend from the pressure, volume, and temperature method.

volume, and temperature estimation using spacecraft telemetry data. The fuel budget analysis was performed before the actual mission operations considering the various nominally expected orbit and attitude maneuvers during the planned mission life. The pressure, volume, and temperature fuel estimation was based on an assumption of the ideal gas behavior of the pressurant gas [19]. The ideal gas law was used to estimate the remaining propellant based on the amount of pressurant that was forced into the propellant tank. The pressure and temperature data were provided from state-of-health telemetry.

Figure 22 shows the remaining fuel trend of the KOMPSAT-I by the pressure, volume, and temperature fuel estimation method. The onboard fuel was used for the four orbit maneuver operations and eight safe-hold mode operations. No fuel has been used since the 23 November 2000. Until now, 30.4% of the fuel has been consumed and the remaining fuel is estimated as 50.45 kg.

## VIII. Orbital Evolution

Osculating to the mean orbit conversion utility was used for monitoring the mean orbital elements of the KOMPSAT-I. The algorithm included the effect of all zonal, sectorial, and tesseral harmonics, second order $J_2$, and third body gravitational perturbations [20]. The altitude of the KOMPSAT-I continuously decreased due to the atmospheric drag, and the inclination also continuously decreased from the gravitational perturbation of the Sun [21]. The atmospheric density varied with the solar activities.

Figure 23 shows the variations of the mean altitude and the solar flux during the three years of the satellite mission operations. The solar flux is the observed values from the National Geophysical Data Center [22]. There have been no orbit maneuvers or safe-hold mode operations since 23 November 2000. Since then, the KOMPSAT-I orbit has naturally evolved. The mean altitude abruptly declined with the rising of the solar flux from 1 September 2001. The mean altitude of the satellite is below the nominal value of 685±1 km. Until now, the altitude raising orbit maneuver has not been performed due to operational inconvenience. Currently the altitude of the KOMPSAT-I is constantly declining by about 20 m/day.

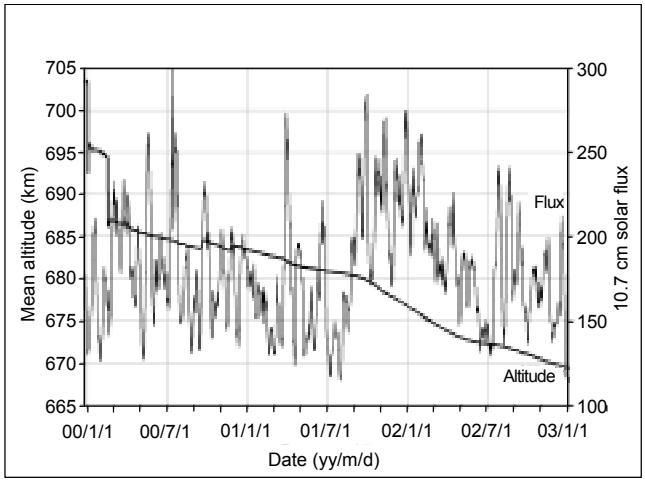


Fig. 23. Variation of the mean altitude and solar flux.

Figure 24 shows the variation of the mean inclination and the shift of the mean local time of the ascending node from the nominal value, i.e., 10:50 AM. Sharp changes of the inclination in LEOP were due to the out-of-plane orbit maneuvers described in the previous section. Slow changes of the inclination were due to the natural gravitational attraction of the Sun. Currently, the local time of the ascending node is constantly delayed but still within the nominal value of 10:50 AM + 10/−15 minutes.

Figure 25 presents the mean argument perigee versus the mean eccentricity diagram. The time variation of the mean eccentricity is also plotted for reference. The orbit of the KOMPSAT-I was in a nearly frozen orbit because of the LEOP orbit maneuver operations [23]. At that time the mean argument of perigee was maintained at 90 ± 13 degrees.

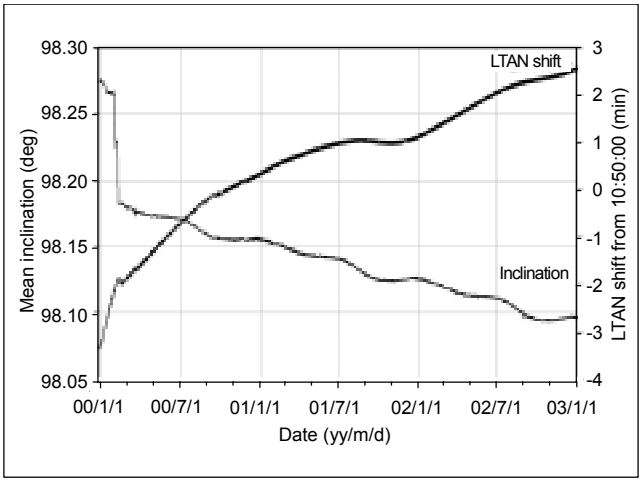


Fig. 24. Variation of the mean inclination and local time of ascending node shift.

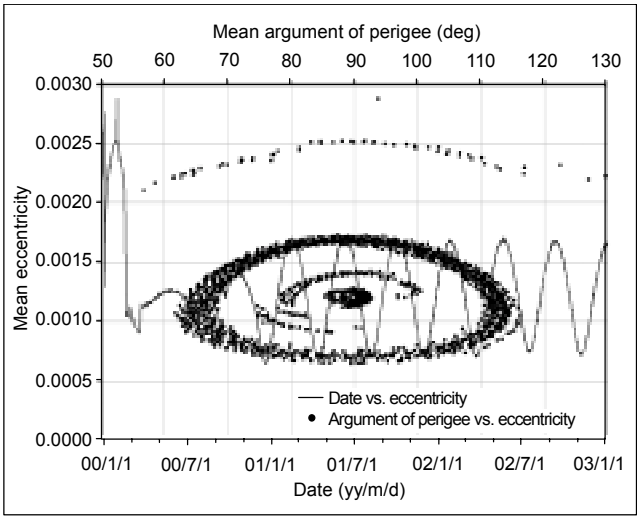


Fig. 25. Variation of the mean eccentricity and argument of perigee.

However, the frozen orbit melted somewhat after the safe-hold mode operations on 23 November 2000. Currently the mean argument of perigee is maintained at 90 ± 25 degrees. The period of the frozen orbit is about 114 days as in the previous study [24].

## IX. Concluding Remarks

This paper reported on the mission operations of the various functions in the mission analysis and planning subsystem (MAPS) for the KOMPSAT-I. The orbit and attitude-related functions were performed for determination and maneuver. We presented the mission scheduling and command planning functions in the imaging operations. We also showed support functions, such as satellite ground track display in a zoomed-in world map, fuel accounting, and osculating-to-mean orbit conversions.

Based on the successful development and operations of the KOMPSAT-I MAPS, more advanced functions and performances will be implemented on the second generation MAPS for the KOMPSAT-II, which is scheduled to be launched in 2004.

## References


[1] J.-W. Eun, J.-I. Choi, W.-S. Choi, W.-C. Jung, and J.-M. Kim, "Architectural Design of KOMPSAT Mission Control Element", *Proc. of 17th AIAA Int'l Commun. Satellite Systems Conf.,* Yokohama, Japan, 1998.

[2] H.-S. Mo, H.-J. Lee, and S.-P. Lee, "Development and Testing of Satellite Operation System for Korea Multipurpose Satellite-I", *ETRI J.,* vol. 22, no. 1, 2000, pp. 1-11.

[3] J.-W. Eun, B.-S. Lee, J.-S. Lee, C.-H. Won, S.-J. Park, Y.-K. Kim, J. Suk, C.-M. Lew, and H.-D. Kim, "Design of Mission Analysis and Planning Software for Korea Multi-Purpose Satellite", *Proc. of Annual Satellite Command, Control and Network Management Conf.,* Reston, VA, USA, 1997.

[4] C.-H. Won, J.-S. Lee, B.-S. Lee, and J.-W. Eun, "Mission Analysis and Planning System for Korea Multipurpose Satellite-I", *ETRI J.,* vol. 21, no. 3, 1999, pp. 29-40.

[5] J.-Y. Kang, J.-M. Kim, and S.-J. Chung, "Design and Development of an Advanced Real-Time Satellite Simulator", *ETRI J.,* vol. 17, no. 3, 1995, pp. 1-16.

[6] W.-S. Choi, S. Lee, J.-W. Eun, H. Choi, and D.-S. Chae, "Design, Implementation and Validation of the KOMPSAT Spacecraft Simulator," *KSAS Int'l J.,* vol. 1, no. 2, 2000, pp. 50-67.

[7] F. R. Hoots and R. L. Roehrich, *Models for propagation of NORAD element sets*, Project Spacecraft Report no. 3, Aerospace Defense Command, U. S. Air Force, 1980.

[8] B.-S. Lee, J.-S. Lee, H.-J. Lee, J.-A. Kim, and H.-J. Choi, "Orbit Determination for the KOMPSAT-I Using GPS Navigation Solutions", *Proc. of the KSAS Spring Conf.,* 2000, pp. 131-134.

[9] Motorola, "VICEROY GPS Spaceborne Receiver", http://www.mot.com/GSS /SSTG/SSSD/Products.html, 2000.
[10] T. Yunck, "Orbit Determination", in *Global Positioning System: Theory and Applications*, ed. by B.W. Parkinson and J.J. Spiler, AIAA, Washington, 1996, pp. 559-592.
[11] O. Montenbruck, E. Gill, and J. M. Fraile-Ordonez, "Orbit Determination of the MIR Space Station Using MOMSNAV GPS Measurements", *Proc. 11th Int'l Astrodynamics Symp.*, paper number 96-c-53, May 19-25, 1996.
[12] SpaceDaily, "Clinton Okays More Accurate GPS Service", http://www.spacedaily.com/news/gps-00d.html, May 10, 2000.
[13] B.-S. Lee, J.-S. Lee, H.-J. Lee, and S.-P. Lee, "Improvement of the KOMPSAT-1 GPS Navigation Solutions After Termination of the Selective Availability", *The 7th GNSS Workshop, Int'l Symp. GPS/GNSS, COEX, Seoul, Korea*, Nov. 30 - Dec. 2, 2000, pp. 36-39.
[14] B.-S. Lee, J.-S. Lee, and J.-A. Kim, "Post Launch Mission Analysis for the KOMPSAT-I", *J. Astronomy & Space Sciences*, vol. 17, no. 2, 2000, pp. 285-294.
[15] M. Duquette, *TAURUS T4 Interim Mission Analysis*, Orbital Science Corporation(OSC), TD-2734, Dulles, Virginia, 1999, pp. 1-19.
[16] B.-S. Lee, S. Lee, H.-J. Lee, J.-A. Kim, E.-K. Kim, and H.-J. Choi, "Near Frozen Orbit Achievement of the KOMPSAT-I Spacecraft", *Proc. the KSAS Spring Conf.*, 2000, pp. 127-130.
[17] H.-D. Kim, H.-J. Choi, and E.-K. Kim, "Mission Planning & Operations for the KOMPSAT-1", *J. Korean Society for Aeronautical and Space Sciences*, vol. 29, no. 6, 2001, pp. 118-126.
[18] Y. Kim, Y. Kim, H.-S. Im, and D. Lee, "KOMPSAT Data Processing System ; An Overview & Preliminary Acceptance Test", *J. Korea Society Remote Sensing*, vol. 5, no. 4, 1999, pp. 357-365.
[19] C. D. Brown, *Spacecraft Propulsion*, AIAA Inc., Washington DC, 1995.
[20] J. R. Guinn, "Periodic Gravitational Perturbations for Conversion Between Osculating and Mean Orbit Elements", *AAS/AIAA Astrodynamics Specialist Conf.*, Durango, Colorado, 1991, AAS Paper 91-430.
[21] B.-S. Lee, "Variations of the Local Time of Ascending Node for the Initial Inclinations of the KOMPSAT", *J. Astronomy & Space Sciences*, vol. 16, no. 2, 1999, pp. 167-176.
[22] NGDC, http://www.ngdc.noaa.gov/stp/SOLAR/FLUX/flux.html.
[23] B.-S. Lee, J.-S. Lee, and J.-H. Kim, "Quick Evaluations of the KOMPSAT-1 Orbit Maneuvers Using Small Sets of Real-Time GPS Navigation Solutions", *Trans. On Control, Automation and Systems Eng.*, vol. 3, no. 3, 2001, pp. 196-202.
[24] B.-S. Lee and J.-S. Lee, "Selection of Initial Frozen Orbit Eccentricity and Evolution of Orbit Due to Perturbations", *J. Korean Society for Aeronautical and Space Sciences*, vol. 25, no. 1, 1997, pp. 126-132.

**Byoung-Sun Lee** received the BS, MS, and PhD degrees in astronomy and space sciences from Yonsei University, Seoul, Korea in 1986, 1988, and 2001. He joined ETRI in 1989, where he was involved in developing the KOREASAT project. From 1992 to 1994, he was an OJT Engineer in Lockheed-Martin Astrospace in the U.S.A. and Martra-Marconi Space in the U.K. for the KOREASAT project. From 1995 to 1999, he participated in the KOMPSAT-1 Ground Mission Control Project as a Senior Member of Research Staff in Mission Analysis and Planning Subsystem. He is now working for the KOMPSAT-2 and COMS-1 Ground Mission Control Project as a Principal Member of Research Staff. His research interests are tracking and orbit determination of satellites and station-keeping maneuvers of collocated geostationary satellites. He is a member of the Korean Space Science Society, Korea Society for Aeronautical and Space Sciences, and ICASE. He is a member of the editorial board in Journal of Astronomy and Space Sciences.

**Jeong-Sook Lee** received the BS and MS degrees in astronomy and space sciences from Yonsei University in 1986 and 1989. She joined ETRI in 1993. She is working for the KOMPSAT-2 Ground Mission Control Project. Her research interests include orbit determination, prediction and control. She is a member of the Korean Space Science Society.

**Jae-Hoon Kim** received the PhD degree in computer engineering from Chungbuk National University, Cheongju, Korea in 2001. He joined ETRI in 1983, where he was involved in developing the Intelligent Network and KOREASAT Projects. From 1992 to 1994, he was an OJT Engineer in Martra-Marconi Space in the U.K. for the KOREASAT Project. From 1995 to 1999, he participated in the KOMPSAT-1 Ground Mission Control Project as a Principle Member of Engineering Staff in System Engineering. He is now working for the KOMPSAT-2 Ground Mission Control Project as Team Leader. His research interests are security in satellite communications, fault diagnosis of satellites using AI technologies, and system modeling using objected-oriented technologies. He is a member of the Korean Space Science Society and Korea Society for Aeronautical and Space Sciences.

**Seong-Pal Lee** received his BS degree in electrical engineering from Seoul National University in 1979. He received the MS and PhD degrees in electrical engineering from Polytechnic Institute of New York, USA, in 1986 and 1990. He joined ETRI in 1980, where he is currently working as a Director of Communications Satellite Development Center, Radio and Broadcasting Research Laboratory. His research interests include satellite communication system, mobile satellite communication service, satellite tracking telemetry & command systems and stratospheric systems.

**Hae-Dong Kim** received the BS and MS degrees in aerospace engineering from Pusan National University, Pusan, Korea in 1994 and 1996. He worked for Hyundai Space & Aircraft Co. from 1996 to 2000 and was involved in developing the KOMPSAT-1 Ground Mission Control Project. He is currently working for Korea Aerospace Research Institute as a Senior Member of Research Staff in the Satellite Mission Operation Department. His research interests are orbit determination, GPS navigation, and mission control systems. He is a member of the Korean Society for Aeronautical and Space Sciences.

**Eun-Kyou Kim** received the BS and MS degrees in aeronautical engineering from Seoul National University, Seoul, Korea. He received the PhD degree in aerospace engineering from the University of Michigan, Ann Arbor, U.S.A. in 1993. He joined KARI in 1995. Since 1999, he has worked for KOMPSAT-1 mission operation. He is a member of the Korea Society for Aeronautical and Space Sciences.

**Hae-Jin Choi** received the PhD degree in aerospace and mechanical engineering from UCLA in 1989. He joined Korea Aerospace Research Institute (KARI) in 1990. From 1993 to 1999, he participated in the KOMPSAT-1 development project as a System Engineer. Since the launch of KOMPSAT-1, he has been in charge of the KOMPSAT-1 operation as the Head of the Satellite Mission Operation Group. He is a member of the Korean Society of Aeronautical & Space Sciences and Korean Space Science Society.